EJN European Journal of Neuroscience

FENS Federation of European Neuroscience Societies

European Journal of Neuroscience, Vol. 39, pp. 2027–2036, 2014 doi:10.1111/ejn.12554

NEUROSYSTEMS

Interneuron firing precedes sequential activation of neuronal ensembles in hippocampal slices

Takuya Sasaki,[1] Norio Matsuki[1] and Yuji Ikegaya[1,2]
[1]Graduate School of Pharmaceutical Sciences, University of Tokyo, Tokyo, Japan
[2]Center for Information and Neural Networks, Suita City, Osaka, Japan

Keywords: circuit, hippocampus, imaging, interneuron, sequence

Abstract

Neuronal firing sequences that occur during behavioral tasks are precisely reactivated in the neocortex and the hippocampus during rest and sleep. These precise firing sequences are likely to reflect latent memory traces, and their reactivation is believed to be essential for memory consolidation and working memory maintenance. However, how the organized repeating patterns emerge through the coordinated interplay of distinct types of neurons remains unclear. In this study, we monitored ongoing spatiotemporal firing patterns using a multi-neuron calcium imaging technique and examined how the activity of individual neurons is associated with repeated ensembles in hippocampal slice cultures. To determine the cell types of the imaged neurons, we applied an optical synapse mapping method that identifies network connectivity among dozens of neurons. We observed that inhibitory interneurons exhibited an increase in their firing rates prior to the onset of repeating sequences, while the overall activity level of excitatory neurons remained unchanged. A specific repeating sequence emerged preferentially after the firing of a specific interneuron that was located close to the neuron first activated in the sequence. The times of repeating sequences could be more precisely predicted based on the activity patterns of inhibitory cells than excitatory cells. In line with these observations, stimulation of a single interneuron could trigger the emergence of repeating sequences. These findings provide a conceptual framework that interneurons serve as a key regulator of initiating sequential spike activity.

Introduction

The reactivation of structured spike patterns in neuronal populations has been assumed to be essential for encoding, consolidation and retrieval of memory in the cortex (O'Neill *et al.*, 2010; Schwindel & McNaughton, 2011). A series of recent studies has demonstrated that the firing sequences that emerge during alert wakefulness are replayed on a millisecond time scale during sharp wave and ripples (SW-Rs) in the hippocampus (Foster & Wilson, 2006; Diba & Buzsaki, 2007; Karlsson & Frank, 2009; Dragoi & Tonegawa, 2011). The repetition of distinct firing modules has also been observed in discharge patterns in the neocortex during transitions from Down to Up states (Luczak *et al.*, 2007), and even in *in vitro* cortical slices (Mao *et al.*, 2001; Ikegaya *et al.*, 2004; MacLean *et al.*, 2005; Matsumoto *et al.*, 2013). Therefore, reactivated patterns are inherent to the cortical network system and could arise from complex interactions between local neuronal ensembles. However, how these specific patterns are created by the dynamic balance between excitatory and inhibitory neuronal activity remains unclear.

In this study, we examined how the timing of repeating sequences is associated with individual spikes by using functional multi-neuron calcium imaging (fMCI), an optical recording technique that monitors neuronal firing based on changes in the somatic fluorescence intensity of a calcium-sensitive indicator (Takahashi *et al.*, 2007; Sasaki *et al.*, 2008). We used a slice culture preparation as our experimental model for the following reasons: (1) it enabled us to record the ongoing activity of hundreds of cells with high spatiotemporal resolution because of low optical scattering (Takahashi *et al.*, 2011); and (2) it preserved the local circuits essential for generating SW-Rs resembling *in vivo* SW-Rs (Maier *et al.*, 2003; Takahashi *et al.*, 2010).

Although the optical imaging technique has revealed multi-neuronal dynamics in various systems (Ikegaya *et al.*, 2004; Ohki *et al.*, 2006; Busche *et al.*, 2008; Bandyopadhyay *et al.*, 2010; Komiyama *et al.*, 2010; Margolis *et al.*, 2012; Ziv *et al.*, 2013), a primary shortcoming of this imaging method is the difficulty in identifying neuronal cell types; excitatory and inhibitory cells cannot be identified by their fluorescence images alone. To circumvent this technical issue, we employed a synapse mapping method termed reverse optical trawling (ROTing), which can identify presynaptic neurons that have monosynaptic connections with patch-clamped neurons (Sasaki *et al.*, 2009; Takahashi *et al.*, 2010). By applying the ROTing method to hippocampal slices, we functionally detected inhibitory neurons in an imaged area and analysed the spatiotemporal activity patterns of excitatory and inhibitory neurons. We discovered that inhibitory neurons increased their firing rates prior to the emergence of repeating sequences, whereas such preceding activity changes were not observed in excitatory pyramidal cells. These results indicate that interneurons provide a temporal fidelity for the sequential activation of ensemble neuronal activity in the cortex.

Correspondence: Dr T. Sasaki, as above.
E-mail: t.sasaki.0224@gmail.com

Received 23 September 2013, revised 5 February 2014, accepted 11 February 2014

Materials and methods

Animal ethics

All experiments were performed with the approval of the animal experiment ethics committee at the University of Tokyo (approval number 19–35), and in accordance with NIH guidelines for the care and use of animals.

Slice preparation

Hippocampal slice cultures were prepared from postnatal day 7 Wistar/ST rats (SLC), as previously described (Koyama *et al.*, 2007). Briefly, rat pups were chilled with ice and decapitated. The brains were removed and cut into 300-μm-thick horizontal slices with a DTK-1500 vibratome (Dosaka, Kyoto, Japan) in aerated, ice-cold Gey's balanced salt solution supplemented with 25 mM glucose. Entorhino-hippocampal stumps were excised and cultured on Omnipore membrane filters (JHWP02500; Millipore, Bedford, MA, USA) that were laid on plastic O-ring disks. The cultures were grown with 1 mL of 50% minimal essential medium, 25% Hank's balanced salt solution and 25% horse serum (Cell Culture Laboratory, Cleveland, OH, USA) in a humidified incubator at 37 ºC in 5% CO_2. The medium was changed every 3.5 days.

Recording ongoing activity with fMCI

On days 6–12 *in vitro*, slices were incubated with 2 mL of dye solution at 37 ºC for 1 h (Takahashi *et al.*, 2007). The dye solution consisted of artificial cerebrospinal fluid (aCSF) containing 0.0005% Oregon Green 488 BAPTA-1 (OGB-1) AM, 0.01% Pluronic F-127 and 0.005% Cremophor EL. The aCSF was composed of (in mM): NaCl, 127; $NaHCO_3$, 26; KCl, 3.3; KH_2PO_4, 1.24; $MgSO_4$, 1.5; $CaCl_2$, 1.5; glucose, 10. After 30 min of recovery, a slice was transferred to a recording chamber and perfused with aCSF at 28–32 ºC at a perfusion rate of 1.5–2.0 mL/min. Fluorophores were excited by the 488-nm line of an argon–krypton laser (5–10 mW, 641-YB-A01; Melles Griot, Carlsbad, CA, USA) and visualized through a 507-nm long-pass emission filter. Images (512 × 512 pixels = 520 × 520 μm, 1-bit intensity) were captured at 50–100 frames/s using a Nipkow-disk confocal scanner unit (CSU-X1; Yokogawa Electric, Tokyo, Japan), cooled CCD camera (iXON DV897; Andor, Belfast, Northern Ireland, UK), upright microscope (ECLIPSE FN1; Nikon, Tokyo, Japan) and water-immersion objective lens (16 × 0.8 NA, CFI75LWD16XW; Nikon). To extract spike activity (Sasaki *et al.*, 2008), the cell bodies of neurons were identified by visual inspection and used to place regions of interest (10-μm-radius circles) in which the fluorescence intensity was averaged across space. For each cell, the change in fluorescence ($\Delta F/F$) was calculated as $(F_t - F_0)/F_0$, where F_t is the fluorescence intensity at any time point and F_0 is the average baseline fluorescence intensity across the 10-s period before and after the focused time point. The onsets of calcium transients were semi-automatically detected using a Matlab program based on principal component analysis and support-vector machines (Sasaki *et al.*, 2008).

Detection of repeating sequences

We used a template-matching algorithm to fully search for repeating sequences (Ikegaya *et al.*, 2004). We first selected cells that exhibited more than one calcium transient. After defining the reference calcium events of the reference cell ($cell_1$), we defined a vector that consisted of a set of cells and the timing of their calcium events relative to the reference events as follows: ($cell_2$, $cell_3$, . . ., $cell_N$, t_2, t_3, . . . t_N), where t_i denotes the delay of the event of $cell_i$ relative to the reference event. t_i was limited to a time window of 500 ms or less. This vector was considered the template and was advanced forward in time through the successive events of $cell_1$ that were recorded over the remainder of the session. If more than two elements were identical between any template pairs, we regarded the matched elements as a repeating sequence. One frame jitter was allowed for detecting repeating sequences. Each mismatched spike configuration was used as another template in a subsequent scan. Thus, every event was included as part of a template sequence, and each template occurred at least once. Data are reported as the mean ± SEM.

Electrophysiological recording

Patch-clamp recordings were performed with a MultiClamp 700B amplifier and a Digidata 1440A digitizer controlled by pCLAMP 10 software (Molecular Devices, Union City, CA, USA). For whole-cell recordings, borosilicate glass pipettes (4–6 MΩ) were filled with an internal solution consisting of (in mM): K-gluconate, 135; KCl, 4; HEPES, 10; phosphocreatine-Na_2, 10; Na_2-GTP, 0.3; Mg-ATP, 4; Alexa Fluor 594 hydrazide, 200 μM (Invitrogen; pH 7.2). Excitatory and inhibitory postsynaptic currents (PSCs) were isolated by clamping at −70 mV and 0 mV, respectively. For loose cell-attached recordings, glass pipettes were filled with aCSF. Signals were low-pass filtered at 1–2 kHz, digitized at 10 kHz, and analysed with pCLAMP 10 software. In some experiments, local field potentials were recorded during fMCI monitoring of the calcium activity of CA3 neurons. Glass pipettes were filled with 2 M NaCl and placed in CA3 stratum pyramidale. To extract the ripple wave activity, the recorded data were band-pass filtered at 150–250 Hz. Ripple-like events were automatically detected based on their oscillatory powers and durations; the root mean square (3-ms window) of the band-passed signal was used to detect the ripple wave with a power threshold of 5 SDs of 10 ms in duration.

Detection of inhibitory neurons by ROTing

To identify presynaptic inhibitory neurons located within an imaging region, we utilized the ROTing technique (Sasaki *et al.*, 2009; Takahashi *et al.*, 2010). After monitoring ongoing activity with calcium imaging as described above, the extracellular solution was changed to modified aCSF, containing (in mM): K^+, 2.2; Mg^{2+}, 3.0; Ca^{2+}, 3.2; to reduce intrinsic activity and the plasticity of the synaptic wiring (Fig. 2). In addition, excitatory neurotransmission was inhibited by applying 50 μM 6-cyano-7-nitroquinoxaline-2,3-dione (CNQX) and 50 μM D,L-2-amino-5-phosphonopentanoic acid (AP5) to block the α-amino-3-hydroxy-5-methyl-4-isoxazolepropionic acid (AMPA)/kainate and *N*-methyl-D-aspartate (NMDA) receptors, respectively. After obtaining whole-cell recordings from one-three pyramidal cells with a holding voltage of 0 mV, another glass pipette (~1 MΩ) filled with 50 mM K^+ in aCSF was placed 20 μm above the surface of the slice, and high K^+ was iontophoretically applied by injecting negative rectangular 3–30 μA currents through the electrode for 1–5 s. The currents were intermittently applied at intervals of 3–5 s to avoid excessive neuronal activation due to the extracellular accumulation of K^+. This procedure evoked calcium transients in a few of the CA3 neurons located within an imaging region. The pipette was slowly moved over the CA3 networks, and the evoked calcium transients were monitored at 50 frames/s. The timings of these events were compared online with PSCs recorded

concurrently in the patch-clamped neurons, and presynaptic inhibitory neurons that were responsible for the focused PSCs were statistically screened. More specifically, for every presynaptic candidate and the frequency of background PSCs, we calculated the probability (P-value) that the observed number of coincident spikes and synaptic currents would occur if they behaved as independent Poisson units (for more detail, see Sasaki *et al.*, 2009). Neurons with a P-value < 0.01 were considered putative presynaptic cells. Using this screen, we detected presynaptic neurons with a false-positive error of $< 1\%$ and a false-negative error of 4% (Sasaki *et al.*, 2009). When a barrage of PSCs with inter-event intervals (IEIs) < 50 ms was observed in the patched neuron, only the first PSC was considered in the analysis, and the subsequent PSCs were ignored because they could have arisen from burst firing in the same presynaptic inhibitory neuron.

Prediction of repeating sequences

We examined whether the activity patterns of individual cells could serve as predictors of the emergence of repeating events. For this purpose, we used a cross-validation analysis in which each dataset was equally divided into two parts; the first part and the last part were used as a training (learning) phase and a test (event detection) phase, respectively. In the training phase, we designated an N-dimensional vector $\vec{X}_t$ (termed prediction vector) that consisted of the ratio of the number of calcium events that occurred from 0 to 100 ms before the onset of sequences to the total event number in individual cells, where N denotes the numbers of recorded neurons. Thus, the prediction vector reflects a series of the prediction probabilities that one sequence emerges 0–100 ms after the calcium events of the corresponding neurons. In the test phase, the prediction vector was used to predict the times of repeating sequences. At a time point t, we designated an N-dimensional vector $\vec{X}_t$ that consisted of the number of calcium events observed during the 100-ms period from $t-100$ (in ms) to t (in ms) in individual neurons. The product $\vec{X}' \vec{P}$ denotes the predicted probability $\vec{P}_{\mathrm{pred}}(t)$ that a sequence may start at the time point t. A predicted event was defined in the case that $\vec{P}_{\mathrm{pred}}$ exceeds 0.5. To quantify the success of the prediction, we calculated the prediction scores, which represent the ratio of the number of the predicted events that correctly coincided with the actual timings of sequence emergence to the total number of predicted events.

Results

Temporally precise sequences of neuronal events

Cortical microcircuits in slice preparations are reported to exhibit precisely timed firing patterns that can be repeated in the same sequential order (Ikegaya *et al.*, 2004; Luczak *et al.*, 2007; Matsumoto *et al.*, 2013). We first confirmed whether precise repetitions of neuronal activity were also emitted by our hippocampal slice culture preparations. We loaded neurons with OGB-1AM and monitored the ongoing activity patterns from 125 ± 6 neurons using fMCI at a frame rate of 50–100 Hz (Fig. 1A; $n = 5$ slices). In this imaging method, the action potentials of a given neuron are measured as transient calcium events in the cell body of the neuron (Fig. 1B). In our imaging condition, the average $\Delta F/F$ amplitude of calcium transients associated with single spikes was $10.4 \pm 2.5\%$, and the signal-to-noise ratio was 11.3 ± 1.5, which allowed us to reliably detect individual single spikes. It should be noted, however, that individual spikes in bursts with a frequency of > 5 Hz were inseparable in fluorescent traces due to the temporal accumulation of calcium transients owing to their slow decay kinetics ($\tau = 400$–600 ms; for more detail, see Sasaki *et al.*, 2008). The length of single movies was $26\,000 \pm 2740$ frames (i.e. 460 ± 67 s). During this imaging period, the percentage of active neurons was $47 \pm 7\%$ and the frequency of neuronal events per cell was 2.0 ± 0.6 min. We used a template matching algorithm that searches for the repeated activation of 'fixed' sequences, which are defined as a subset of neurons that fire sequentially with the same order and the same delay. We referred to these precise repetitions as repeating sequences. In each dataset, a diverse repertoire of repeating sequences was detected (an example is shown in Fig. 1C and D). Single sequences appeared 2.6 ± 0.2 times (range, two-eight times; $n = 1051$ sequences from five slices), and $42.0 \pm 3.9\%$ of calcium events participated in at least one sequence ($n = 8846$ events from five slices). To evaluate the significance of sequence emergence, the number of repeating sequences in the physiological datasets was compared with those in surrogate datasets. Here, we employed two shuffling methods: (1) IEIs were randomly shuffled within each cell; and (2) single events of two randomly selected cells were repeatedly exchanged (Ikegaya *et al.*, 2004; Sasaki *et al.*, 2007). IEI shuffling eliminates the temporal correlation among cell populations but preserves the firing rates of individual neurons, whereas event pair exchange eliminates the precise orders of active cells but preserves the firing rates of individual neurons and the times of global population activity. For each original dataset, 20 surrogates were created (Fig. 1C, right). In all slices tested, significantly fewer repeating sequences were found in surrogate datasets; the real-to-surrogate ratios of the number of neurons involved in a single repeating sequence were 2.4 ± 0.2 and 2.2 ± 0.2 in IEI shuffling and event pair exchange methods, respectively, which were significantly higher than 1 (IEI shuffling, $P = 0.016$, $t_4 = 3.05$, paired t-test; event pair exchange, $P = 0.010$, $t_4 = 4.61$). This value increased as the number of neurons increased (Fig. 1E), which indicates that repeating sequences with larger numbers of neurons emerged with higher fidelity. Simultaneous recordings of extracellular signals and population events demonstrated that repeating sequences were associated with ripple oscillations that were detected by filtering CA3 local field potentials at 150–250 Hz (Fig. 1F and G). Overall, 32% of repeating sequences were correlated with the timing of ripple oscillations. The mean duration of the sequences was 163 ± 83 ms; this time scale is in accordance with *in vivo* observations that behavioral sequences in hippocampal place cells are replayed within a time window of hundreds of milliseconds during SW-Rs (Foster & Wilson, 2006; Diba & Buzsaki, 2007; Karlsson & Frank, 2009; Dragoi & Tonegawa, 2011).

Identifying inhibitory neurons by ROTing

Having statistically confirmed the occurrence of repeating sequences, we next examined how the repeating sequences are coordinated by excitatory and inhibitory neuronal populations. To identify inhibitory interneurons in an imaging region, we applied the ROTing technique, a modified method from reverse optical probing (Aaron & Yuste, 2006), which searches for presynaptic neurons by simultaneously monitoring the firing activity of individual neurons and PSCs from patch-clamped neurons (Sasaki *et al.*, 2009). The concept of ROTing is illustrated in Fig. 2A–E; if neuron A repeatedly displays calcium events that are time-locked to the timing of inhibitory PSCs recorded from neuron B, neuron A is a putative presynaptic interneuron that sends inhibitory inputs to neuron B. We have previously shown that this method can detect presynaptic neurons

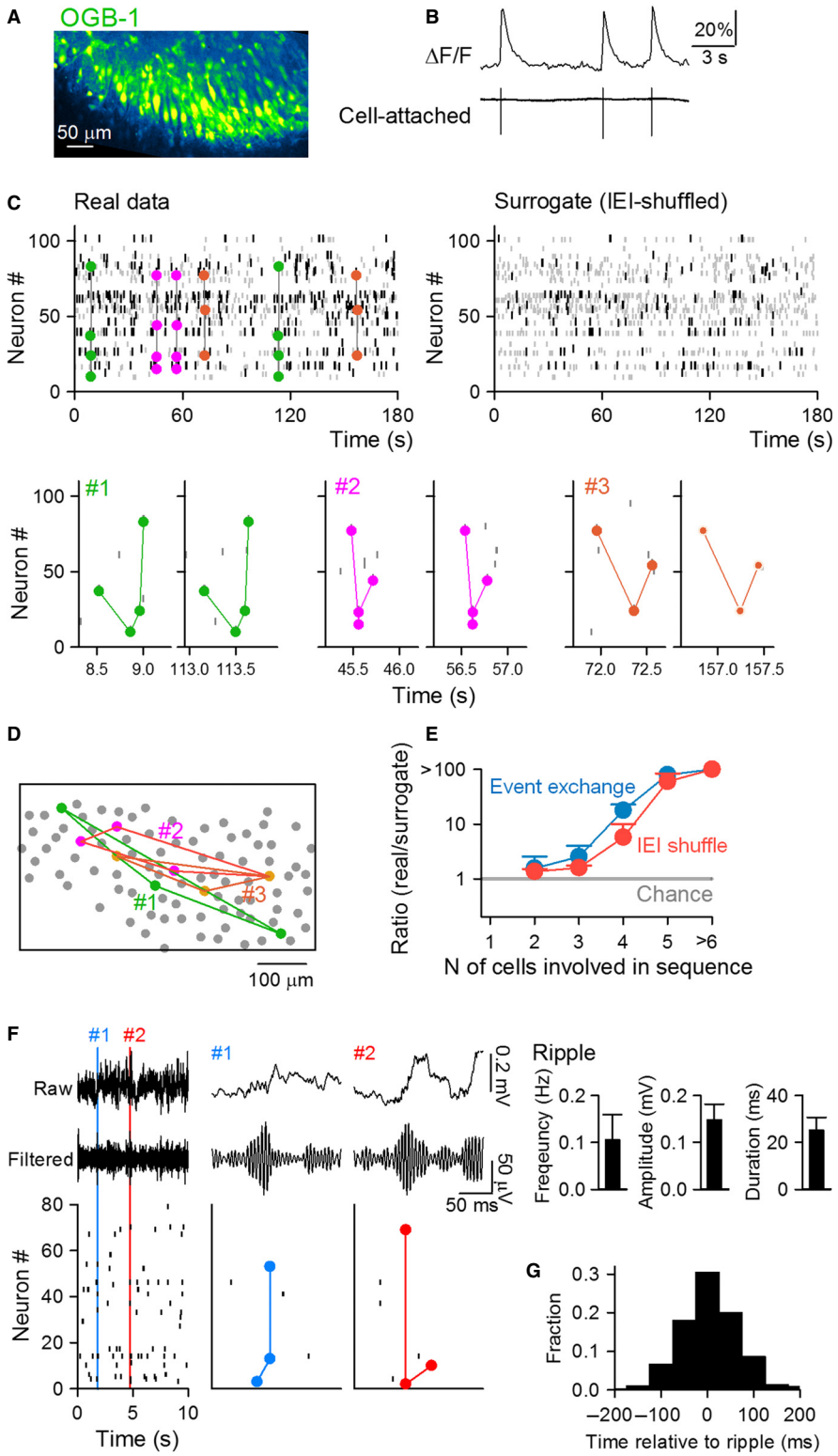

FIG. 1. Statistical salience of repeating sequences in ongoing network activity. (A) Confocal image of a hippocampal slice loaded with OGB-1. (B) Simultaneous recordings of somatic calcium signals sampled at a frame rate of 50 Hz (top) and juxtacellular currents (bottom) from the same neuron indicate that calcium transients reflect the firing of action potentials. (C) A sample rastergram showing repeating sequences. Each dot represents a single calcium event. Events involved and not involved in sequences are shown as black and gray dots, respectively. Three representative repeating sequences are shown as connected lines and magnified in time in the three bottom panels. The right panel shows a surrogate rastergram generated by the IEI-shuffling procedure. (D) The locations of the cells in the sequences shown in (C). (E) The average ratios of the number of sequences in real datasets to those in 20 surrogate datasets (n = 5 slices) are plotted as a function of the number of neurons involved in sequences. (F) Simultaneous recordings of CA3 local field potentials band-pass filtered at 150–250 Hz (top) and activity patterns of the neuronal population (bottom). Two representative ripple events are magnified in the right insets, depicting sequence emergence corresponding with the timing of ripple generation. Right bar graphs show the basic properties of ripples (n = 154 ripples from five slices). (G) Cross-correlogram of repeating sequences with CA3 ripple events (n = 108).

with a 1% false-positive error rate (Sasaki *et al.*, 2009). As shown in Fig. 2A, we first monitored ongoing network activity under conditions of (in mM): K^+, 4.2; Mg^{2+}, 1.5; Ca^{2+}, 1.5, for 10 min to detect relay sequences. We then changed the extracellular solution to the modified aCSF (in mM: K^+, 2.2; Mg^{2+}, 3.0; Ca^{2+}, 3.2). This procedure was employed to minimize spontaneous activity and synaptic transmission failure, and thereby increase the fidelity of ROTing. After the network stabilization, we clamped two-five neurons at a holding potential of 0 mV to record inhibitory PSCs, and monitored the spatiotemporal firing patterns of neurons using fMCI (Fig. 2B). To improve detection accuracy, we conducted whole-cell recordings from two-five neurons that were located at an inter-cell distance of > 50 μm. A cocktail of ionotropic glutamate receptor antagonists, CNQX and AP5, was applied so that PSCs reflected inhibitory activities more faithfully. Under these conditions, we applied 50 mM K^+ through a glass pipette and induced calcium events in a small fraction of neurons. The pipette was slowly moved over the pyramidal cell layer to equally activate as many neurons as possible (Fig. 2C). Some calcium events in different neurons coincided during relatively short time periods, but most of them were not fully synchronized and were separable. We analysed the relative timing between calcium events of individual neurons and inhibitory PSCs of the patched neurons, and determined putative inhibitory neurons that projected to the patch-clamped neuron. In the example data shown in Fig. 2D, the timings of the calcium events of neuron #37 coincided significantly with the timings of PSCs, with a *P*-value < 0.01, which indicates that this neuron could be a presynaptic cell candidate that transmits inhibitory transmission to the patched neuron. By applying this analysis to all imaged neurons, we defined the positions of putative inhibitory cells. The ratio of putative inhibitory neurons to total active neurons was 19.1 ± 1.8% (n = 295 active cells from five slices). This fraction is in agreement with the estimation that the overall proportion of interneurons in the hippocampal pyramidal cell layer is ~20% (Freund & Buzsaki, 1996). Based on the offline identification of putative excitatory and inhibitory cells, we separately reconstructed their ongoing activity patterns (Fig. 2F) that were recorded before application of ROTing (for procedure, see Fig. 2A). The frequency of spontaneous activity of inhibitory neurons was slightly higher than that of excitatory neurons, but the difference was not statistically significant (Fig. 2G).

Inhibitory neurons are active before repeating sequences

We then investigated how excitatory and inhibitory neurons are engaged in the sequential events. The ratios of the number of events participating in sequences to the total number of events were 41.8 ± 3.9% and 35.8 ± 8.8% in excitatory (n = 515 cells) and inhibitory (n = 54 cells) cells, respectively. To examine the activity changes before and after the appearance of repeating sequences, we aligned rastergrams of population activity to the onset of individual sequences (Fig. 3A). The resulting peri-event time histogram revealed that the firing rates of inhibitory cells increased progressively before the emergence of repeating sequences; the mean calcium event frequency of inhibitory cells increased significantly by 510% during a period of 20–100 ms before the onset of repeating sequences (Fig. 3B; P = 0.031, t_4 = 3.24, paired-t test, n = 54 cells from five slices). In contrast, no elevation of the firing rate occurred in excitatory cells (P > 0.05, n = 515 cells). Once sequences started, excitatory and inhibitory neurons showed 3.4 and 4.5 times increases in their firing rates, respectively (P < 0.05, Tukey's test after ANOVA). These firing rate changes resembled those observed during SW-Rs (Csicsvari *et al.*, 1999, 2000; Klausberger *et al.*, 2003).

We analysed the activity patterns of individual inhibitory cells and identified interneurons that were specifically activated before individual sequences (Fig. 3C). We observed that the same inhibitory neurons tended to be activated prior to the emergence of identical sequences (Fig. 3D). The probability that a sequence was repeatedly preceded by the same inhibitory cell was significantly higher than the probability that a sequence was preceded by different inhibitory cells (Fig. 3D; P = 0.042, t_4 = 2.95, paired t-test). To examine the spatial relationship of the pre-activated interneurons and the subsequent relay sequences, we measured the cell-to-cell distance between the neuron activated first in a sequence and the interneuron that fired ahead of the sequence (Fig. 3E). The mean distance was 61.3 ± 2.4 μm, which was significantly smaller than that obtained from 100 surrogate datasets (Fig. 3F; $P = 1.3 \times 10^{-8}$, D_{1385} = 0.20, Kolmogorov–Smirnov test). The surrogates were generated by random shuffling of the cell identity within each cell map. These results suggest that the generation of repeated sequences was determined by the firing of specific interneurons that were located close to the initiation sites of the sequences.

To further verify the relevance of the selective increase in firing rates in inhibitory cells, we determined if the activity patterns of individual cells can predict the sequence-onset times. In each cell type, we created a vector (prediction vector) that represented the ratios of the number of calcium events that preceded any sequences by 0–100 ms to the number of total events in individual cells (Fig. 4A). The ratio represents the prediction probability that one sequence emerges 0–100 ms after the calcium event of each neuron. Typically, inhibitory cells showed higher probabilities than excitatory cells. Then, the likelihood of the emergence of a repeating sequence was calculated at every instantaneous time by defining the prediction scores as the ratio of the number of correctly predicted events to the total number of predicted events. The prediction scores obtained from inhibitory cells were significantly higher than those from excitatory cells and those of inhibitory cells in IEI-shuffled datasets (Fig. 4B; P < 0.05, Tukey's test, n = 5). Thus, compared with excitatory cells, the activity patterns of inhibitory cells provided a better prediction for sequence emergence.

Next, we examined the firing properties of interneurons with a prediction probability of > 0.20 (termed here 'trigger interneurons'). Based on the temporal patterns of calcium events, individual trigger interneurons were classified into three cell types: oscillatory cells (type 1); bursty cells (type 2); and random firing cells (type 3). Oscillatory cells were defined as cells in which the coefficient of variation of IEIs was < 0.6. Bursty cells were defined as cells in which 40% of the IEIs were < 1 s. Random firing cells were defined as cells that were not classified into the above two types. Out of 20 trigger interneurons, six cells and 10 cells were found to be oscillatory and bursty cells, respectively (Fig. 4C). This result suggests that both firing types are likely to contribute to the generation of repeating sequences.

Activation of a single interneuron can trigger repeating sequences

In order to clarify the causal influence of interneurons on the emergence of repeating sequences, we tested whether stimulation of an interneuron could trigger repeating sequences in surrounding neurons. An anatomically identified interneuron was whole-cell recorded and spike trains were repeatedly evoked while monitoring population activity by fMCI (Fig. 5B). In five cells out of 10 cells recorded, phasic stimulation (200 pA, 500 ms) at a frequency of 0.1 Hz increased the frequency of repeating sequences by

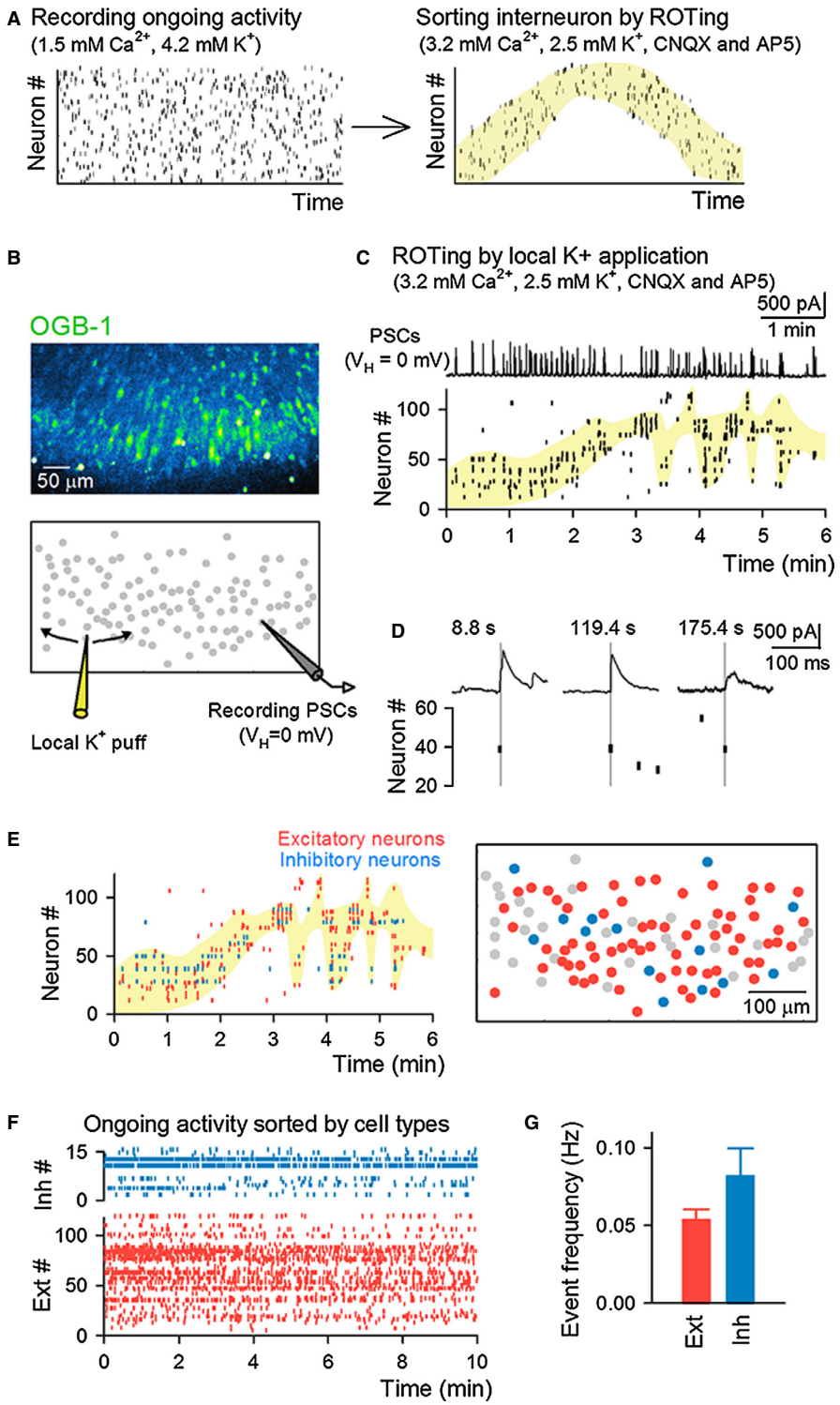

FIG. 2. Mapping of inhibitory neurons in the hippocampal CA3 region. (A) Schematic illustration of the experimental procedure. After recording ongoing activity patterns using fMCI (left), the ionic composition of the aCSF was modified to 3.2 mM Ca^{2+} and 2.2 mM K^+, and ionotropic glutamate receptor antagonists (CNQX and AP5) were added. Then, reverse optical trawling (ROTing) was performed to identify interneurons (right). (B) Confocal image of a hippocampal slice loaded with OGB-1 (top); 125 neurons were searched for inhibitory synaptic connections (bottom). A few neurons were activated by the local application of K^+ through a glass pipette (yellow pipette), which was manually moved over the network. The evoked activity patterns were monitored using fMCI, and inhibitory PSCs were recorded from one-three CA3 pyramidal cells in whole-cell configuration at a holding potential of 0 mV. (C) PSCs in a patched neuron (top) and the spatiotemporal pattern of the calcium events of 125 neurons (bottom) in response to K^+ application. Each dot represents a single calcium event. The shaded area indicates the regions activated during movement of the K^+ pipette. (D) Typical events in (C). In this case, the calcium events of neuron #37 were time-locked to PSC onsets, and thus this neuron was identified as a presynaptic cell candidate that innervated the patched neuron. (E) Calcium events of putative excitatory and inhibitory neurons in the same plot shown in (C) (left). The locations of these cells are shown in the cell map (right). Neurons that did not exhibit activity during ROTing are shown in light gray. (F) A typical rastergram of ongoing calcium events of 110 putative excitatory and 15 inhibitory neurons. (G) The mean frequency of calcium events of 515 excitatory and 54 inhibitory cells. Error bars are SEM.

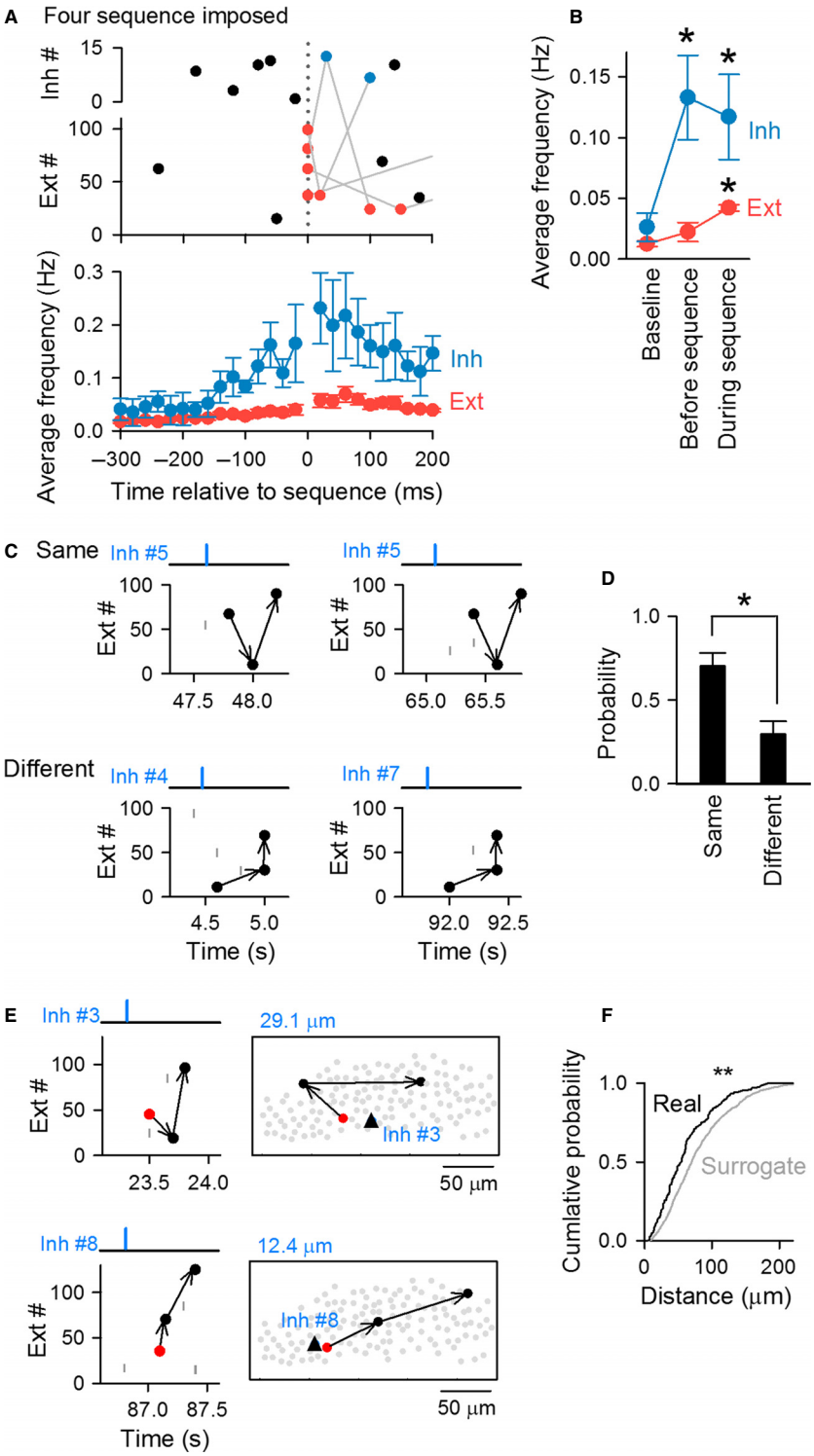

FIG. 3. Sequence-preceding activation of inhibitory neurons. (A) (top) Four representative repeating sequences (gray lines) were aligned to the timing of their first activities in the sequences. Unconnected plots (Smith *et al.*, 2004) represent events not involved in sequences. (Bottom) Peri-event time histogram summarizing the changes in the mean firing rates of 515 excitatory and 54 inhibitory cells relative to the onset of repeating sequences. (B) The average event frequencies at baseline (Baseline), 20–100 ms before each sequence (Before sequence), and during the repeating sequences (During sequence). Error bars are SEM. $*P < 0.05$, Tukey's test after one-way ANOVA. (C) Representative sequences preceded by the same inhibitory cell #5 (top, same), or different cells #4 and #7 (bottom, different). Calcium event onsets of the focused inhibitory cells are shown in blue on the top of the corresponding rastergrams. Neuronal events involved and not involved in sequences are shown in black and gray, respectively, in the rastergrams. Relay sequences are indicated by the arrows. (D) The probabilities that repeating sequences are preceded by the same or different inhibitory cells are compared. Error bars are SEM. $*P < 0.05$, paired *t*-test. (E) Two examples of repeating sequences and the spatial arrangements of the participating neurons. The inhibitory cells activated before the sequences are shown in the triangle. (F) The cumulative probability distribution of the cell-to-cell distances between the first active cells in individual sequences and the inhibitory cells that were activated before the emergence of the sequences is compared with that in 100 surrogates, which were generated by random shuffling of the cell identity in the same cell map. $**P < 0.01$, Kolmogorov–Smirnov test.

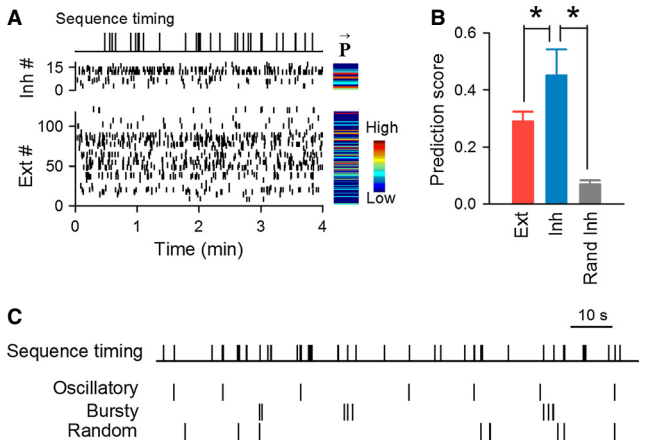

FIG. 4. Prediction of the occurrence of repeating sequences by interneuron firing. (A) The timing of individual repeating sequences (top) was extracted from the rastergram (bottom). Gray-scale images (right) show the prediction vector $P^{\rightarrow}$ for the rastergram, which represents the percentage of the events detected 0–100 ms before sequence emergence in each cell. (B) The mean prediction scores are compared between excitatory and inhibitory cells. The score calculated from IEI-shuffled activity in inhibitory cells is shown in gray. Error bars are SEM. $^*P < 0.05$, Tukey's test after ANOVA. (C) Times of repeating sequences (top) and calcium events of representative oscillatory, bursty and random firing interneurons (bottom).

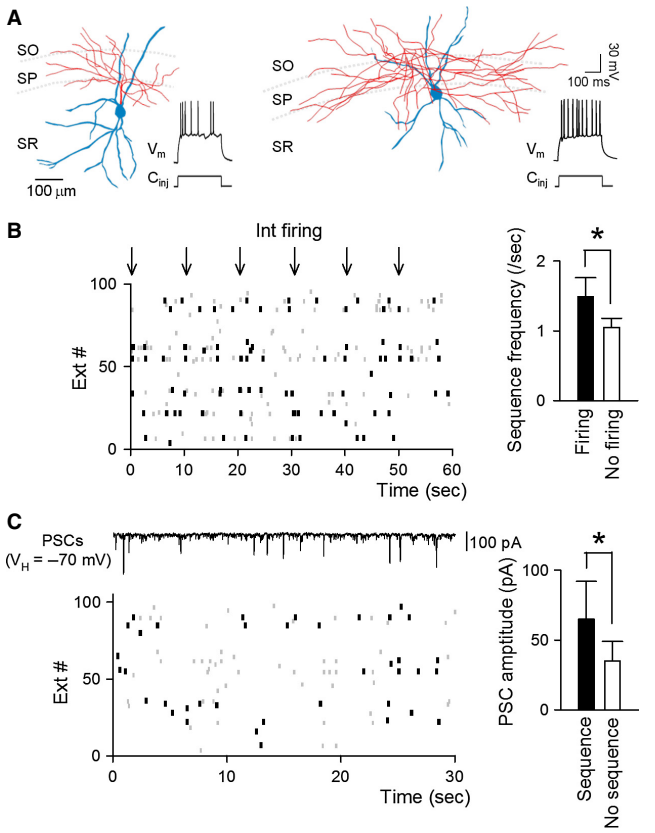

FIG. 5. Stimulation of an interneuron can trigger repeating sequences. (A) Representative reconstruction of two interneurons as visualized with Alexa 568 labeling on a schematic representation of the hippocampus. Only the main dendrites and axon fibers are illustrated. The typical voltage trace in response to a suprathreshold current pulse (200 pA) is shown in the right inset. (B) Simultaneous current injection of the interneuron shown in (A, left) and optical imaging of population activity by fMCI. The frequency of sequences increased in phase with the times of interneuronal firing (arrows). Events involved and not involved in sequences are shown as black and gray dots, respectively. The right panel shows the frequency of sequences with and without the interneuronal firing. Error bars are SEM. $^*P < 0.05$, paired *t*-test. (C) Simultaneous voltage-clamp recording of an interneuron (top, $V_H = -70$ mV) combined with fMCI (bottom). The right panel shows the amplitude of PSCs 0–500 ms before the emergence of repeating sequences (sequence). The average amplitudes in other periods are shown as 'No sequence'. Error bars are SEM. $^*P < 0.05$, paired *t*-test.

125–220% within 500 ms after the interneuron firing ($P = 0.038$, $t_4 = 3.06$, paired *t*-test). These cells that were successful in triggering sequences show fast-spiking or non-fast-spiking responses to current injection (Fig. 5A). Both types possessed multipolar dendrites and exhibited dense preferential innervation of the CA3 principal cell layer, suggesting a perisomatic interneuron subtype (Fig. 5A). Voltage-clamp recordings revealed that these successful neurons received strong PSCs prior to the onset of sequence occurrence (Fig. 5C; $P = 0.039$, $t_4 = 3.03$, paired *t*-test). These results suggest that a subset of hippocampal interneurons receive strong synaptic inputs that drive their spikes preceding repeating sequences, which in turn determines active cell patterns in the following sequences.

Discussion

Recent advances in multi-channel unit recordings from behaving animals have revealed that distinct subsets of neurons are repeatedly activated during both waking and sleep; this repeated activation could underlie memory consolidation and retrieval (O'Neill *et al.*, 2010; Carr *et al.*, 2011; Schwindel & McNaughton, 2011). In the present work, we took advantage of functional optical imaging and analysed the temporal relationships between the emergence of repeating sequences and individual spikes. We discovered that inhibitory interneurons, rather than excitatory pyramidal cells, exhibited an enhanced activity level before the initiation of repeating sequences. Moreover, we observed that pre-activated interneurons were located in the vicinity of the neurons that were activated first in sequences.

Hippocampal interneurons *in vivo* preferentially discharge action potentials in discrete time windows relative to the timing of SW-Rs, suggesting unique roles in synchronous network oscillations (Ylinen *et al.*, 1995; Klausberger *et al.*, 2003). Parvalbumin-expressing basket cells increase their firing rates during SW-Rs (Lapray *et al.*, 2012). The activation of perisomatic-targeting interneurons is sufficient to trigger SW-Rs by controlling the balance between excitatory and inhibitory inputs in a subpopulation of pyramidal neurons (Ellender *et al.*, 2010). Additionally, the firing of axo-axonic cells, which exclusively target the pyramidal cell axon initial segment, is transiently enhanced at the beginning of SW-Rs and strongly suppressed during SW-Rs (Klausberger *et al.*, 2003; Viney *et al.*, 2013). Taken together, these stereotyped inhibitory cells may collaboratively provide conditions permissive for the initiation of SW-Rs. In addition to this notion, our findings indicate that inhibitory neurons play a crucial role not only in triggering the flow of network oscillations but also in creating precise repeating sequences in hippocampal circuits.

The frequency of ripple oscillations in cultured slices was 0.10 ± 0.05 Hz (Fig. 1F), and lower than those reported in acute slice preparations (≥ 0.5 Hz; Maier *et al.*, 2003; Wu *et al.*, 2005; Norimoto *et al.*, 2012; Hajos *et al.*, 2013). It was rather comparable to the frequency observed in *in vivo* animals, ranging from 0.05 to 0.5 Hz. This might be owing to the recovery of connectivity among neurons in culture. In addition, acute slice preparations require a

high perfusion rate (3–15 mL/min) for metabolic supply to generate SW-Rs, whereas the perfusion rate of 1.5–2.0 mL/min was sufficient to obtain SW-Rs in our cultured slices. Therefore, mechanisms underlying SW-Rs in cultured slices might differ from those in acute slices. To extrapolate our results to *in vivo* brain functions, further experimental work will be required using an advanced experimental approach.

The emergence of repeating sequences has been theoretically predicted by the synfire chain hypothesis (Abeles, 1991), which posits that the precisely timed reactivation of distinct neuronal subsets propagates through neural networks (Diesmann *et al.*, 1999). Such precise firing sequences have been verified in recent decades (Prut *et al.*, 1998; Mao *et al.*, 2001; Ikegaya *et al.*, 2004; Luczak *et al.*, 2007). However, the existence of reactivated patterns with millisecond precision has been called into question by the claim that repeating patterns in spike trains (Baker & Lemon, 2000; Oram *et al.*, 2001) and membrane potential fluctuations (Mokeichev *et al.*, 2007) could occur by chance. This contradiction arises from different assumptions for creating surrogates to be compared with the original datasets. In general, too strong statistical assumptions cause false-negative detection of sequences and tend to lead to a conclusion against the existence of sequences. In fact, neuronal networks are non-randomly woven by synaptic connections (Song *et al.*, 2005; Yoshimura *et al.*, 2005; Yu *et al.*, 2009). Because in the biological system the function is tightly coupled to the structure, it is a natural consequence that functional activities emitted by a non-randomly structured neuronal network are non-randomly patterned in space and time. We thus suspect that the failure to reject the null hypothesis against the sequence existence in several studies is simply due to inappropriate statistical assumptions for data surrogates.

The contributions of inhibitory circuits to the regulation of repeating sequences are attributable to a variety of physiological principles at the single-cell level. One of the most likely mechanisms is that inhibitory inputs reset the regular firing of principal cells that are not originally a part of the sequence, and delay their firing to enable their participation in a later phase of the sequence. On a millisecond time scale, feed forward interneurons preserve the temporal fidelity of synaptic integration and action potential generation in pyramidal cells (Pouille & Scanziani, 2001; Lamsa *et al.*, 2005). In addition to such inhibitory effects, interneurons can elicit a post-inhibitory rebound depolarization, which in turn is capable of triggering an action potential or a short burst of spikes within a restricted time window (Lytton & Sejnowski, 1991; Buzsaki & Chrobak, 1995; Cobb *et al.*, 1995; Ellender *et al.*, 2010). Assuming that numerous pyramidal cells share the common subthreshold influence of a single presynaptic interneuron (Freund & Buzsaki, 1996; Fino & Yuste, 2011), the synergistic effects of phase resetting and depolarizing overshoot could powerfully regulate the dynamics of neuronal ensembles. In line with this prediction, a recent paper has demonstrated that the activation of single inhibitory neurons can more effectively induce synchronous activity patterns in the developing hippocampus (Bonifazi *et al.*, 2009) and animal behavioral responses (Houweling & Brecht, 2008) than the activation of excitatory principal cells. Taken together, we suggest that inhibitory interneurons perform the dynamic selection and control of precisely timed replay in neuronal ensembles, leading to information transfer, memory formation and retrieval in the cortex.

Acknowledgements

This work was partly supported by Grants-in-Aid for Science Research on Innovative Areas, ‘Mesoscopic Neurocircuitry’ (no. 22115003), from the Ministry of Education, Culture, Sports, Science and Technology of Japan, and by the Funding Program for Next Generation World-Leading Researchers (LS023).

Abbreviations

aCSF, artificial cerebrospinal fluid; AP5, D,L-2-amino-5-phosphonopentanoic acid; CNQX, 6-cyano-7-nitroquinoxaline-2,3-dione; fMCI, functional multineuron calcium imaging; IEI, inter-event interval; OGB-1, Oregon Green 488 BAPTA-1; PSC, postsynaptic current; ROTing, reverse optical trawling; SW-R, sharp wave and ripple.

References

Aaron, G. & Yuste, R. (2006) Reverse optical probing (ROPING) of neocortical circuits. *Synapse*, **60**, 437–440.

Abeles, M. (1991) *Corticonics: Neural Circuits of the Cerebral Cortex*. Cambridge University Press, Cambridge, MA.

Baker, S.N. & Lemon, R.N. (2000) Precise spatiotemporal repeating patterns in monkey primary and supplementary motor areas occur at chance levels. *J. Neurophysiol.*, **84**, 1770–1780.

Bandyopadhyay, S., Shamma, S.A. & Kanold, P.O. (2010) Dichotomy of functional organization in the mouse auditory cortex. *Nat. Neurosci.*, **13**, 361–368.

Bonifazi, P., Goldin, M., Picardo, M.A., Jorquera, I., Cattani, A., Bianconi, G., Represa, A., Ben-Ari, Y. & Cossart, R. (2009) GABAergic hub neurons orchestrate synchrony in developing hippocampal networks. *Science*, **326**, 1419–1424.

Busche, M.A., Eichhoff, G., Adelsberger, H., Abramowski, D., Wiederhold, K.H., Haass, C., Staufenbiel, M., Konnerth, A. & Garaschuk, O. (2008) Clusters of hyperactive neurons near amyloid plaques in a mouse model of Alzheimer’s disease. *Science*, **321**, 1686–1689.

Buzsaki, G. & Chrobak, J.J. (1995) Temporal structure in spatially organized neuronal ensembles: a role for interneuronal networks. *Curr. Opin. Neurobiol.*, **5**, 504–510.

Carr, M.F., Jadhav, S.P. & Frank, L.M. (2011) Hippocampal replay in the awake state: a potential substrate for memory consolidation and retrieval. *Nat. Neurosci.*, **14**, 147–153.

Cobb, S.R., Buhl, E.H., Halasy, K., Paulsen, O. & Somogyi, P. (1995) Synchronization of neuronal activity in hippocampus by individual GABAergic interneurons. *Nature*, **378**, 75–78.

Csicsvari, J., Hirase, H., Czurko, A., Mamiya, A. & Buzsaki, G. (1999) Oscillatory coupling of hippocampal pyramidal cells and interneurons in the behaving Rat. *J. Neurosci.*, **19**, 274–287.

Csicsvari, J., Hirase, H., Mamiya, A. & Buzsaki, G. (2000) Ensemble patterns of hippocampal CA3-CA1 neurons during sharp wave-associated population events. *Neuron*, **28**, 585–594.

Diba, K. & Buzsaki, G. (2007) Forward and reverse hippocampal place-cell sequences during ripples. *Nat. Neurosci.*, **10**, 1241–1242.

Diesmann, M., Gewaltig, M.O. & Aertsen, A. (1999) Stable propagation of synchronous spiking in cortical neural networks. *Nature*, **402**, 529–533.

Dragoi, G. & Tonegawa, S. (2011) Preplay of future place cell sequences by hippocampal cellular assemblies. *Nature*, **469**, 397–401.

Ellender, T.J., Nissen, W., Colgin, L.L., Mann, E.O. & Paulsen, O. (2010) Priming of hippocampal population bursts by individual perisomatic-targeting interneurons. *J. Neurosci.*, **30**, 5979–5991.

Fino, E. & Yuste, R. (2011) Dense inhibitory connectivity in neocortex. *Neuron*, **69**, 1188–1203.

Foster, D.J. & Wilson, M.A. (2006) Reverse replay of behavioural sequences in hippocampal place cells during the awake state. *Nature*, **440**, 680–683.

Freund, T.F. & Buzsaki, G. (1996) Interneurons of the hippocampus. *Hippocampus*, **6**, 347–470.

Hajos, N., Karlocai, M.R., Nemeth, B., Ulbert, I., Monyer, H., Szabo, G., Erdelyi, F., Freund, T.F. & Gulyas, A.I. (2013) Input-output features of anatomically identified CA3 neurons during hippocampal sharp wave/ripple oscillation *in vitro*. *J. Neurosci.*, **33**, 11677–11691.

Houweling, A.R. & Brecht, M. (2008) Behavioural report of single neuron stimulation in somatosensory cortex. *Nature*, **451**, 65–68.

Ikegaya, Y., Aaron, G., Cossart, R., Aronov, D., Lampl, I., Ferster, D. & Yuste, R. (2004) Synfire chains and cortical songs: temporal modules of cortical activity. *Science*, **304**, 559–564.

Karlsson, M.P. & Frank, L.M. (2009) Awake replay of remote experiences in the hippocampus. *Nat. Neurosci.*, **12**, 913–918.

Klausberger, T., Magill, P.J., Marton, L.F., Roberts, J.D., Cobden, P.M., Buzsaki, G. & Somogyi, P. (2003) Brain-state- and cell-type-specific firing of hippocampal interneurons *in vivo*. *Nature*, **421**, 844–848.

Komiyama, T., Sato, T.R., O'Connor, D.H., Zhang, Y.X., Huber, D., Hooks, B.M., Gabitto, M. & Svoboda, K. (2010) Learning-related fine-scale specificity imaged in motor cortex circuits of behaving mice. *Nature*, **464**, 1182–1186.

Koyama, R., Muramatsu, R., Sasaki, T., Kimura, R., Ueyama, C., Tamura, M., Tamura, N., Ichikawa, J., Takahashi, N., Usami, A., Yamada, M.K., Matsuki, N. & Ikegaya, Y. (2007) A low-cost method for brain slice cultures. *J. Pharmacol. Sci.*, **104**, 191–194.

Lamsa, K., Heeroma, J.H. & Kullmann, D.M. (2005) Hebbian LTP in feed-forward inhibitory interneurons and the temporal fidelity of input discrimination. *Nat. Neurosci.*, **8**, 916–924.

Lapray, D., Lasztoczi, B., Lagler, M., Viney, T.J., Katona, L., Valenti, O., Hartwich, K., Borhegyi, Z., Somogyi, P. & Klausberger, T. (2012) Behavior-dependent specialization of identified hippocampal interneurons. *Nat. Neurosci.*, **15**, 1265–1271.

Luczak, A., Bartho, P., Marguet, S.L., Buzsaki, G. & Harris, K.D. (2007) Sequential structure of neocortical spontaneous activity *in vivo*. *Proc. Natl. Acad. Sci. USA*, **104**, 347–352.

Lytton, W.W. & Sejnowski, T.J. (1991) Simulations of cortical pyramidal neurons synchronized by inhibitory interneurons. *J. Neurophysiol.*, **66**, 1059–1079.

MacLean, J.N., Watson, B.O., Aaron, G.B. & Yuste, R. (2005) Internal dynamics determine the cortical response to thalamic stimulation. *Neuron*, **48**, 811–823.

Maier, N., Nimmrich, V. & Draguhn, A. (2003) Cellular and network mechanisms underlying spontaneous sharp wave-ripple complexes in mouse hippocampal slices. *J. Physiol.*, **550**, 873–887.

Mao, B.Q., Hamzei-Sichani, F., Aronov, D., Froemke, R.C. & Yuste, R. (2001) Dynamics of spontaneous activity in neocortical slices. *Neuron*, **32**, 883–898.

Margolis, D.J., Lutcke, H., Schulz, K., Haiss, F., Weber, B., Kugler, S., Hasan, M.T. & Helmchen, F. (2012) Reorganization of cortical population activity imaged throughout long-term sensory deprivation. *Nat. Neurosci.*, **15**, 1539–1546.

Matsumoto, K., Ishikawa, T., Matsuki, N. & Ikegaya, Y. (2013) Multineuronal spike sequences repeat with millisecond precision. *Front. Neural. Circuits*, **7**, 112.

Mokeichev, A., Okun, M., Barak, O., Katz, Y., Ben-Shahar, O. & Lampl, I. (2007) Stochastic emergence of repeating cortical motifs in spontaneous membrane potential fluctuations *in vivo*. *Neuron*, **53**, 413–425.

Norimoto, H., Mizunuma, M., Ishikawa, D., Matsuki, N. & Ikegaya, Y. (2012) Muscarinic receptor activation disrupts hippocampal sharp wave-ripples. *Brain Res.*, **1461**, 1–9.

Ohki, K., Chung, S., Kara, P., Hubener, M., Bonhoeffer, T. & Reid, R.C. (2006) Highly ordered arrangement of single neurons in orientation pinwheels. *Nature*, **442**, 925–928.

O'Neill, J., Pleydell-Bouverie, B., Dupret, D. & Csicsvari, J. (2010) Play it again: reactivation of waking experience and memory. *Trends Neurosci.*, **33**, 220–229.

Oram, M.W., Hatsopoulos, N.G., Richmond, B.J. & Donoghue, J.P. (2001) Excess synchrony in motor cortical neurons provides redundant direction information with that from coarse temporal measures. *J. Neurophysiol.*, **86**, 1700–1716.

Pouille, F. & Scanziani, M. (2001) Enforcement of temporal fidelity in pyramidal cells by somatic feed-forward inhibition. *Science*, **293**, 1159–1163.

Prut, Y., Vaadia, E., Bergman, H., Haalman, I., Slovin, H. & Abeles, M. (1998) Spatiotemporal structure of cortical activity: properties and behavioral relevance. *J. Neurophysiol.*, **79**, 2857–2874.

Sasaki, T., Matsuki, N. & Ikegaya, Y. (2007) Metastability of active CA3 networks. *J. Neurosci.*, **27**, 517–528.

Sasaki, T., Takahashi, N., Matsuki, N. & Ikegaya, Y. (2008) Fast and accurate detection of action potentials from somatic calcium fluctuations. *J. Neurophysiol.*, **100**, 1668–1676.

Sasaki, T., Minamisawa, G., Takahashi, N., Matsuki, N. & Ikegaya, Y. (2009) Reverse optical trawling for synaptic connections *in situ*. *J. Neurophysiol.*, **102**, 636–643.

Schwindel, C.D. & McNaughton, B.L. (2011) Hippocampal-cortical interactions and the dynamics of memory trace reactivation. *Prog. Brain Res.*, **193**, 163–177.

Smith, A.C., Frank, L.M., Wirth, S., Yanike, M., Hu, D., Kubota, Y., Graybiel, A.M., Suzuki, W.A. & Brown, E.N. (2004) Dynamic analysis of learning in behavioral experiments. *J. Neurosci.*, **24**, 447–461.

Song, S., Sjostrom, P.J., Reigl, M., Nelson, S. & Chklovskii, D.B. (2005) Highly nonrandom features of synaptic connectivity in local cortical circuits. *PLoS Biol.*, **3**, e68.

Takahashi, N., Sasaki, T., Usami, A., Matsuki, N. & Ikegaya, Y. (2007) Watching neuronal circuit dynamics through functional multineuron calcium imaging (fMCI). *Neurosci. Res.*, **58**, 219–225.

Takahashi, N., Sasaki, T., Matsumoto, W., Matsuki, N. & Ikegaya, Y. (2010) Circuit topology for synchronizing neurons in spontaneously active networks. *Proc. Natl. Acad. Sci. USA*, **107**, 10244–10249.

Takahashi, N., Oba, S., Yukinawa, N., Ujita, S., Mizunuma, M., Matsuki, N., Ishii, S. & Ikegaya, Y. (2011) High-speed multineuron calcium imaging using Nipkow-type confocal microscopy. *Curr. Protoc. Neurosci.*, **2**, 2.14.

Viney, T.J., Lasztoczi, B., Katona, L., Crump, M.G., Tukker, J.J., Klausberger, T. & Somogyi, P. (2013) Network state-dependent inhibition of identified hippocampal CA3 axo-axonic cells *in vivo*. *Nat. Neurosci.*, **16**, 1802–1811.

Wu, C., Asl, M.N., Gillis, J., Skinner, F.K. & Zhang, L. (2005) An *in vitro* model of hippocampal sharp waves: regional initiation and intracellular correlates. *J. Neurophysiol.*, **94**, 741–753.

Ylinen, A., Bragin, A., Nadasdy, Z., Jando, G., Szabo, I., Sik, A. & Buzsaki, G. (1995) Sharp wave-associated high-frequency oscillation (200 Hz) in the intact hippocampus: network and intracellular mechanisms. *J. Neurosci.*, **15**, 30–46.

Yoshimura, Y., Dantzker, J.L. & Callaway, E.M. (2005) Excitatory cortical neurons form fine-scale functional networks. *Nature*, **433**, 868–873.

Yu, Y.C., Bultje, R.S., Wang, X. & Shi, S.H. (2009) Specific synapses develop preferentially among sister excitatory neurons in the neocortex. *Nature*, **458**, 501–504.

Ziv, Y., Burns, L.D., Cocker, E.D., Hamel, E.O., Ghosh, K.K., Kitch, L.J., Gamal, A.E. & Schnitzer, M.J. (2013) Long-term dynamics of CA1 hippocampal place codes. *Nat. Neurosci.*, **16**, 264–266.